Springer

KSME

Journal of Mechanical Science and Technology 24 (2010) 441~450
www.springerlink.com/content/1738-494x
DOI 10. 1007/s12206-009-1107-8

A numerical study on the flow and mixing in a microchannel using magnetic particles †

Thanh Nga Le, Yong Kweon Suh and Sangmo Kang*

Department of Mechanical Engineering, Dong-A University, Saha-gu, Busan, 604-714, Korea

(Manuscript Received August 24, 2009; Revised September 16, 2009; Accepted September 16, 2009)

Abstract

We have numerically investigated the characteristics of the flow and mixing in a microchannel using magnetic particles. The main flow is driven by the pressure gradient along the channel, while the secondary flow for the mixing is induced by the drag forces of the particles. Here, the particles can move in the flow due to the strong attraction under the periodically-varying magnetic field generated by electromagnets. For the study, the fractional step method based on the finite volume method is used to obtain the velocity field of the fluid and the trajectories of the particles. This study aims at achieving good mixing by periodically changing the direction of magnetic actuation force in time to activate the interaction between the particles and the flow. The quality of mixing is estimated by considering the mixing index and Poincaré section. In this study, parameter studies on the switching frequency, the magnetic actuation force, the number of magnetic particles and so on are performed to understand their effects on the flow and mixing. Results show that the clustering of magnetic particles during the magnetic actuation plays an important part in good mixing. It is also found that the magnetic force magnitude and switching frequency are the two main parameters that make a combined influence on the mixing efficiency. Such a mixing technique using magnetic particles would be an alternative, effective application for the flow and mixing in a microchannel.

Keywords: Microchannel; Mixing Index; Magnetic Force; Magnetic Particles; Poincaré Section

1. Introduction

Recently the biological and chemical analyses in microfluidic systems have been widely used and developed for many applications. Chemical reactions, bio-analytical techniques and so on used in these analyses need a rapid, efficient mixing process. Although the mixing can be carried out easily at a macroscale due to the turbulence, the mixing at a microscale at low Reynolds number, Re (less than 100), is a big challenge for researchers due to the dominating molecular diffusion. To obtain a full mixing at a microscale, therefore, the microchannel has to be extended extremely long.

To achieve faster mixing with a shorter channel, two kinds of mixers are used: passive and active. The main mechanism for good mixing in a microscale is to enlarge the contact surface between different fluids and shorten the diffusion path between them. In passive mixers [1], the mixing is obtained without any external power, for example by using serpentine, herringbone, T-shape and Y-shape channels, which split the main flow into many subsequent flows and then achieve the chaotic advection flow pattern. In active micromixers [2-9], on the other hand, the chaotic advection is created by applying an external power. Active mixers can be sorted into the following, according to the time-dependent disturbance field: pressure gradient, thermal, acoustic, electro-hydrodynamic, dielectrophoretic, electro-kinetic and magneto-hydrodynamic disturbances. A number of research works have been reported regarding both active and passive mixing in the literature, and both of them have advantages and disadvantages in themselves. Although passive mixers are preferred due to their easy fabrication and integration in the actual micro system, active mixers are more investigated so far because they can produce excellent mixing under the condition of short channel and limited time.

Unlike the other active micromixers, only recently has the magnetic particle based micromixer been invented. Magnetic particles had been mainly applied to biomedical and biological researches [10-12] such as cell separation, drug delivery and hyperthermia treatment before the advent of the micromixer. For the present decade, the particles have been also exploited in the mixing performance. First, Rida et al. [2] performed an experimental study, where 95% of mixing efficiency was achieved within 400 μm length in a micromixer. Subsequently, Suzuki et al. [3] investigated the active mixing by utilizing

† This paper was recommended for publication in revised form by Associate Editor Dongshin Shin

*Corresponding author. Tel.: +82 51 200 7636, Fax.: +82 51 200 7656
E-mail address: kangsm@dau.ac.kr.

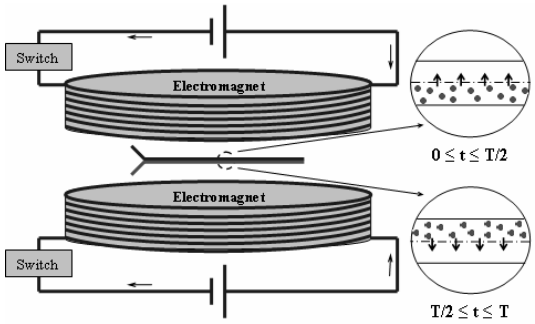

Fig. 1. Conceptual diagram of magnetic micromixer. Here, T is the time period of magnetic actuation.

magnetic beads in a two-dimensional serpentine microchannel. They revealed the mechanism for creating stretching and folding of the lump of magnetic beads, leading to efficient mixing. In the study, they performed numerical analysis employing the superposition method and compared the result with the experimental one. The comparison showed their poor agreement but similar tendency. Using the same numerical method with Suzuki et al. [3], Zolgharni et al. [4] presented a magnetic micromixer with serpentine conductors. They obtained a mixing efficiency of about 85% in a 500 μm mixing-length channel with the extremely small average flow velocity. Recently, Wang et al. [5] reported a numerical study on a micromixer using magnetic particles. In particular, they solved the fluid flow and the motion of magnetic particles simultaneously, unlike the superposition method employed by Suzuki et al. [3] and Zogharni et al. [4]. However, they did not mention clearly any primary mechanism for efficient mixing.

To clarify the main mechanism on which the mixing process is based, in this paper, we have taken account of an active mixer with magnetic particles inserted in the microchannel flow. The magnetic mixer is based conceptually on the magnetic properties of magnetic particles that are attracted by external magnets. The alternate switching of the currents through the electromagnets in the first and second half-periods, as shown in Fig. 1, induces the chaotic motion of magnetic particles and then the vortex motion of the fluid, resulting in mixing in a microchannel. Based on this primary principle, we have investigated a magnetic mixer to bring high performance of mixing. The purpose of this study is to reveal the mixing mechanism of the micromixer and evaluate the effects of the switching frequency, the magnetic force magnitude, the number of magnetic particles, the Péclet number and the initial condition of the concentration distribution on the mixing efficiency. Through this study, we can clearly understand the mixing mechanism, which has not been reported so far in literature, making the present study different from other existing ones.

2. Numerical method

In this study, we consider a simple microchannel, as shown in Fig. 1, where an incompressible fluid flows together with

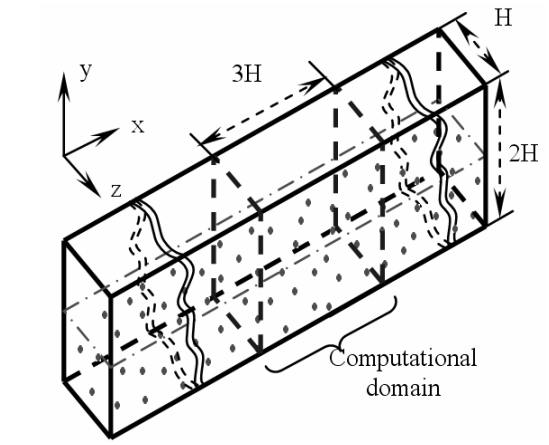

Fig. 2. Schematic diagram of the non-dimensional computational domain (H=1).

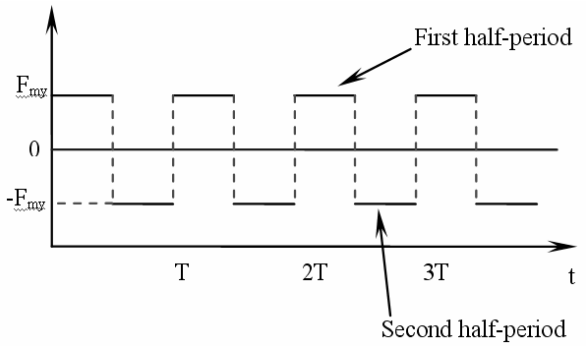

Fig. 3. Time trace of the magnetic force exerted on each particle.

magnetic particles. Fig. 2 shows a schematic diagram illustrating the flow geometry and the computational domain. The fluid flow and the particle motion are solved by employing the same numerical method used in Wang et al. [5].

The magnetic particles in a fluid under the external magnetic field are exerted by several forces: magnetic force, drag force, particle-particle interactions, inertia, gravity and thermal kinetics. To facilitate the numerical simulation, we are interested only in the mixing effect due to the magnetic and drag forces. For the motion of the magnetic particles, therefore, the classical non-dimensional Newtonian equation is used as follows:

$$m_p \frac{du_{p,i}}{dt} = -F_{d,i} + F_{m,i}, \tag{1}$$

where m_p and $u_{p,i}$ are, respectively, the mass and velocity of the particle, and $F_{m,i}$ and $F_{d,i}$ are respectively the magnetic and drag forces. In this study, we assume that the magnetic field becomes uniform and dominant in the vertical (y) direction [5] because of the very large-sized electromagnets compared with the microchannel. By alternately switching the currents on/off through the magnets, the time-dependent disturbance can be created as depicted in Fig. 3. Fig. 3 shows the time trace of the magnetic force exerted on each particle. In the

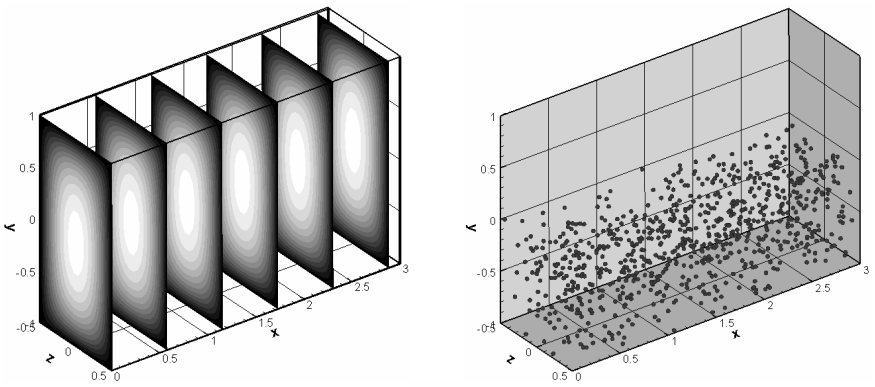

(a) (b)

Fig. 4. Initial condition of (a) the streamwise velocity field and (b) the distribution of magnetic particles in the microchannel.

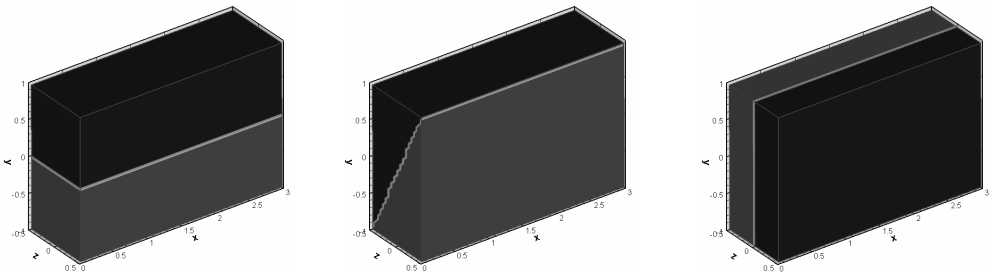

(a) (b) (c)

Fig. 5. Initial conditions of the scalar-concentration distribution in the microchannel: C=0 (black color) for the buffer and C=1 (gray color) for the sample. (a) horizontal case, (b) diagonal case and (c) vertical case.

first half-period, the upper magnet becomes activated and the lower one becomes inactive, generating a magnetic force in the upper direction ($+F_{my}$). In the second half-period, on the other hand, the magnetic force is exerted in the lower direction ($-F_{my}$).

The incompressible flow in the microchannel can be described by the following non-dimensional momentum equations:

$$\frac{\partial u_i}{\partial t}+\frac{\partial u_i u_j}{\partial x_j}=-\frac{\partial p}{\partial x_i}-\frac{12}{\mathrm{Re}}\delta_{i1} +\frac{1}{\mathrm{Re}}\frac{\partial^2 u_i}{\partial x_j \partial x_j}+f_d\delta\left(\mathbf{r},\mathbf{r}_p\right), \tag{2}$$

$$\frac{\partial u_j}{\partial x_j}=0, \tag{3}$$

where u_i is the flow velocity, p is the pressure, Re is the Reynolds number, and $f_d\delta$ (r, r_p) is an external force exerted on the particle, here, the drag force. In addition, δ (r, r_p) is the Dirac delta function ($\delta=0$ except r= r_p) and rp denotes the particle position. The main flow in the microchannel is driven by the constant pressure gradient, 12/Re.

The mixing quality can be described by the diffusive-convective equation for the scalar concentration distribution in the microchannel as follows:

$$\frac{\partial C}{\partial t}+\frac{\partial C u_j}{\partial x_j}=\frac{1}{\mathrm{Pe}}\frac{\partial^2 C}{\partial x_j \partial x_j}, \tag{4}$$

where C is the concentration and Pe is the Peclet number.

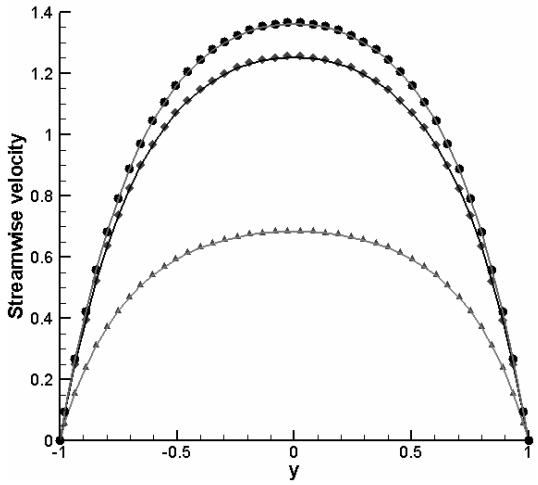

Fig. 6. Streamwise velocity as a function of y at different z positions from the wall. The numerical solutions at z=-0.355 (Δ), z=-0.145 (◊), z=-0.029 (○) are compared with the corresponding analytical ones (solid lines).

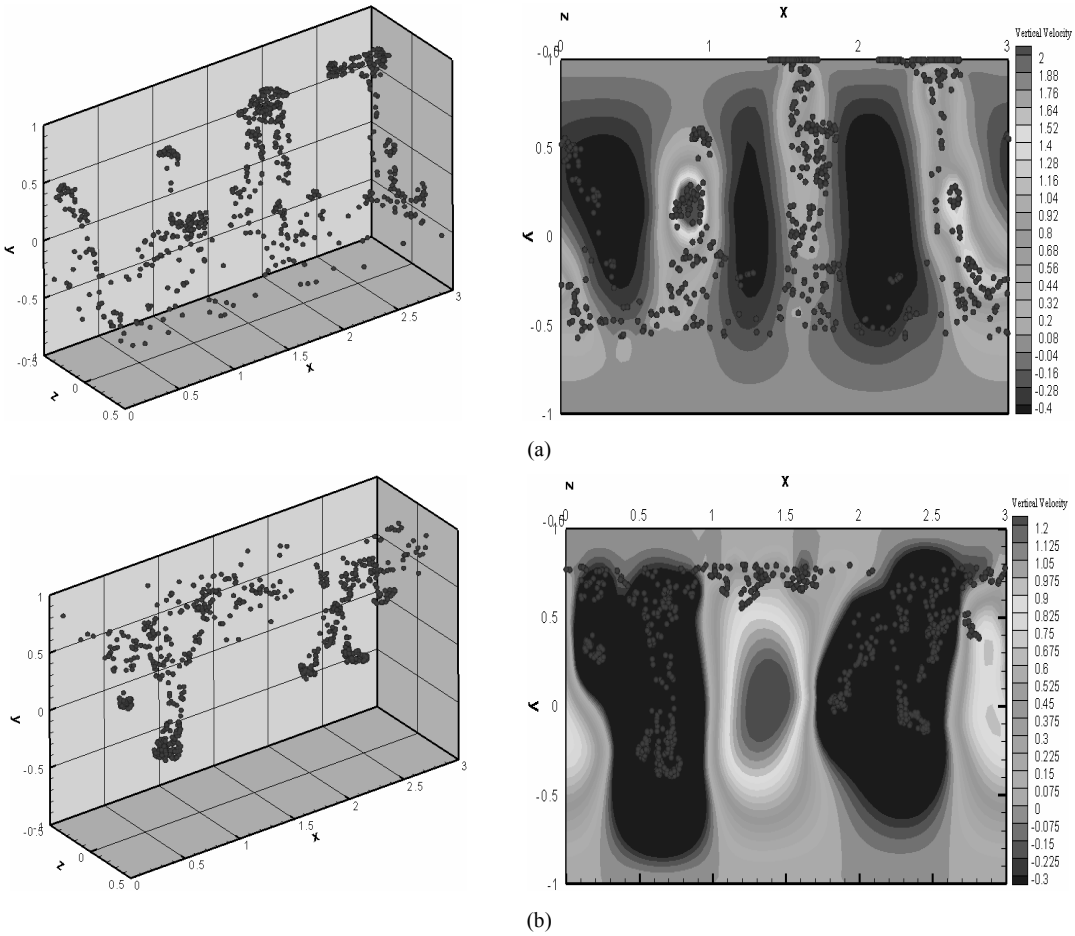

Fig. 7. Particle distributions (left plots) and contour of the vertical velocity (v) in the xy plane (z=0.175) (right plots) at t= (a) 10.4 (in the first half-period) and (b) 15.2 (in the second half-period) for F_m=4, f=0.3 and N_p=800.

Here, we set the concentration distribution of $C=1$ for the sample and $C=0$ for the buffer as the initial condition.

Note that all the variables used in this study are non-dimensionalized by the channel half-height ($H=100\mu m$), the average main flow velocity ($U_0=1mm/s$), the fluid viscosity ($\upsilon=10^{-6}m^2/s$), the density of fluid ($\rho_f=1000kg/m^3$), the particle radius ($R_p=0.5\mu m$) and the density of magnetic particle ($\rho_p=1580kg/m^3$). The governing equations are spatially discretized by using the second-order central difference scheme on a staggered mesh with the number of grid points 60x40x20. The semi-implicit fractional step method with a third-order Runge-Kutta scheme for the body force term and a second-order Crank-Nicolson scheme for the diffusion term is used to integrate the Navier-Stokes equation and the particle motion equation in time. After the discretization, the algebraic equations of the Navier-Stokes equations are solved by using ICCG (Incomplete Cholesky conjugate gradient) method. To examine the mixing process, in this study, three kinds of complementary simulations are employed to make the mixing mechanism in the microchannel clearly understood: concentration field, mixing index and Poincaré section.

On the channel walls, no-slip boundary condition ($u_i=0$) is used for the velocity components and the zero gradient condition is for the concentration ($\partial C/\partial y=0$, $\partial C/\partial z=0$). Periodic boundary condition is imposed on the velocity components ($u_{i,out}=u_{i,in}$) and concentration ($C_{out}=C_{in}$) in the streamwise (x) direction. For the initial condition, the fully developed flow is set for the flow field (see Fig. 4(a)) while three kinds of distribution are for the scalar concentration (see Fig. 5). The magnetic particles are injected uniformly onto the sample in the lower half part of the microchannel as shown in Fig. 4(b). The initial velocity of each magnetic particle is assumed equal to the velocity of the fluid flow $u_{p,i}=u_i\delta$ (r, r_p).

To validate the numerical method, we compare the numerical streamwise velocity in the microchannel with the analytical one achieved from the following equation [13]:

$$u(y,z)=u_{\max}\left[1-(2z)^2+\sum_{n=1}^{\infty}(-1)^n\frac{32}{(2n-1)^3\pi^3}\times\cos\left((2n-1)\pi z\right)\frac{\cosh\left((2n-1)\pi(y)\right)}{\cosh\left(2(2n-1)(\pi/2)\right)}\right] \quad (5)$$

Fig. 6 shows the streamwise (x) velocity as a function of y

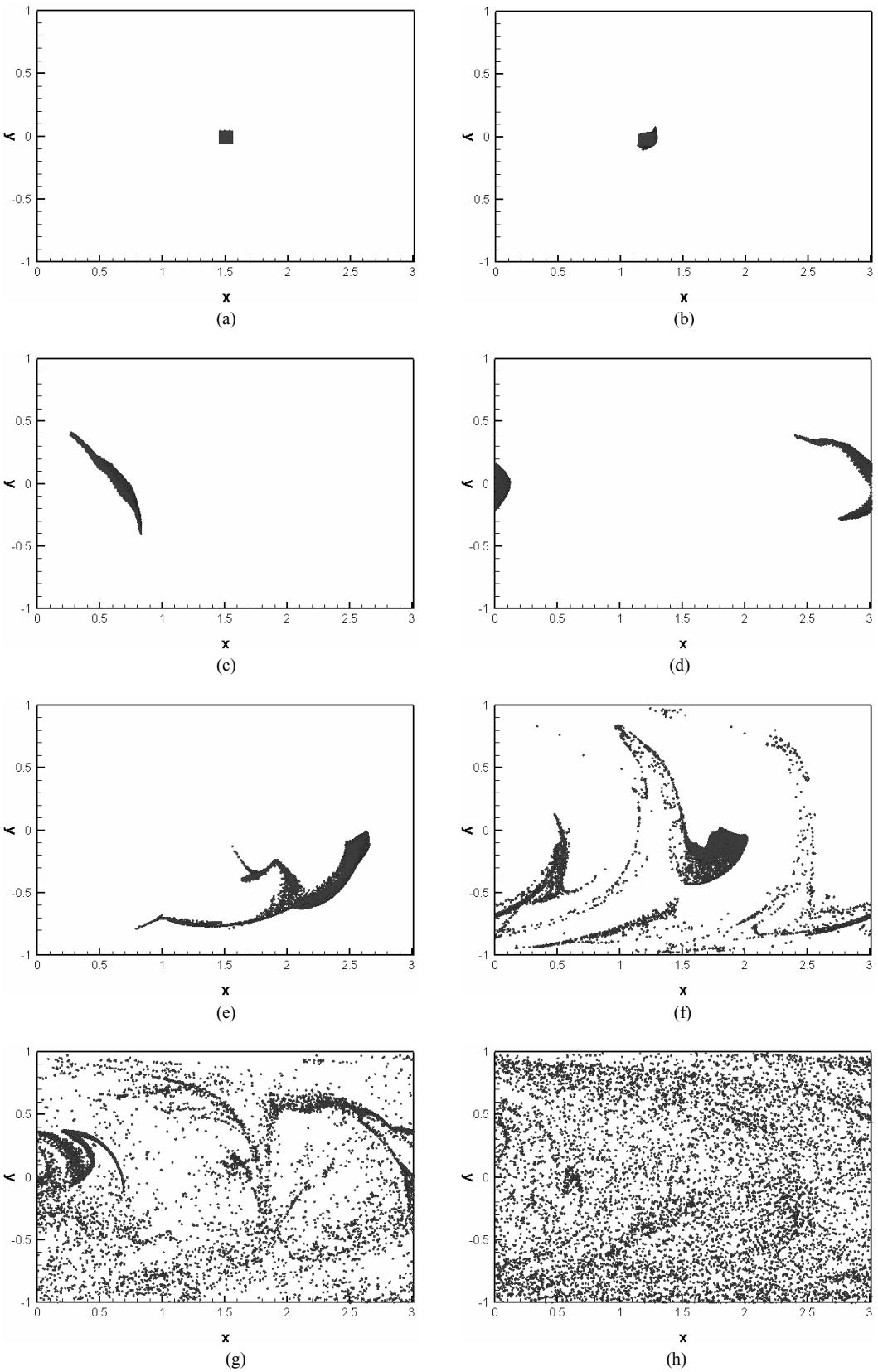

Fig. 8. Evolution of the Poincaré section in time for F_m=4, f=0.3 and N_p=800: t= (a) 0, (b) 2, (c) 6, (d) 10, (e) 14, (f) 18, (g) 26, (h) 40.

at different z positions from the walls. The numerical solutions are in good agreement with the analytical ones for the number of grid points 60x40x20. Therefore, these resolutions are used through the present study.

3. Results and discussion

3.1 Mixing mechanism by the magnetic actuation

3.1.1 Particle-distribution pattern

In this section, the numerical results are illustrated in detail. When the magnetic particles are scattered in the microchannel without any application of external magnetic field, they follow the fluid flow and thus distribute themselves randomly without mixing, as shown in Fig. 4(b). When, however, the actuation magnetic force varying in time is applied (see Fig. 3), the magnetic particles are alternately magnetized and then attracted by the magnets, thus traveling up in the first half-period and down in the second half-period. The magnetic particles forced by the magnetic field move toward the wall, thus leading to accumulate there and create some chains composed of a large number of clustered magnetic particles after some periods of manipulation, as shown in Fig. 7 for instance. These chains agitate the flow up and down, causing the vortex motion of the fluid needed for the mixing. Fig. 7 shows particle distributions and contours of the vertical velocity in the xy plane at two different instants after some periods: one is in the first half-period and the other is in the second half-period. The figure clearly indicates the effect of the chains of magnetic particles on the flow field. In the first half-period, the magnetic particles go up, together with the fluid surrounding them, but the fluid between those chains moves in the opposite direction because of the flow continuity. This phenomenon creates vertical vortex flow, implying a good mechanism for the mixing. In the second half-period, the same phenomenon can also be observed. That is, these phenomena repeat in time and accelerate the mixing.

3.1.2 Poincaré section

The mixing mechanism can be evaluated more clearly by computing the Poincaré section. To achieve the Poincaré section in the microchannel, 8000 passive fluid particles are placed uniformly in a 0.1x0.1x0.1 cubic blob located at $d\mathbf{r}/dt=\mathbf{v}(\mathbf{r},t)$, where $\mathbf{r}(t)=x(t)\mathbf{i}+y(t)\mathbf{j}+z(t)\mathbf{k}$ is the fluid-particle position. Here, the fluid velocity $\mathbf{v}(\mathbf{r},t)$ can be obtained by tri-linear interpolation from the nodal values of the velocity cells. By using the fourth-order Runge-Kutta method, the fluid-particle position can be estimated and projected on the xy plane.

If the fluid particles occupy the whole xy plane in the Poincaré section regardless of the initial position, it can be said that chaotic mixing is achieved.

Fig. 8 shows the Poincaré section for the cubic blob plotted at t = 0, 2, 6, 10, 14, 18, 26, and 40. The folding and stretching illustrated clearly from the deformation of the cubic blob (see Fig. 8) can exhibit the mixing mechanism. The cubic blob is stretched first by the streamwise fluidic flow, as shown in Fig. 8(a)-(d). When the magnetic particles are accumulated together enough to create some chains of magnetic particles (see Fig. 7), the fluid flow between those chains becomes accelerated in the backward direction, inducing the big folding, as shown in Fig. 8(e)-(g). Then the folded chains are stretched by the central flow with the higher velocity and then narrowed again by the slower-velocity flow near the walls. This process repeats, leading to manifest chaotic mixing. Eventually, a good mixing pattern is created with the uniform distribution of the fluid particles, as shown in Fig. 8(h).

3.2 Parametric studies

To evaluate exactly the mixing performance together with the concentration field and Poincaré section, another parameter could also be employed, the so called mixing index *I* defined as

$$I = \frac{1}{\bar{C}}\sqrt{\frac{1}{N}\sum_{i}^{N}\left(C_i - \bar{C}\right)^2}, \tag{6}$$

where $\bar{C}$ is the average concentration in the computational domain, defined as $\bar{C} = \sum C_i/N$ (i=1, N). Here, C_i is the concentration at each grid point and N is the total number of grid points in the region. Note that the decrease of the mixing index means the increase in the mixing performance.

3.2.1 Effect of Péclet number

In terms of the mixing index, the effect of the Péclet number (Pe=U_0H/D) on the mixing efficiency is investigated for three cases of Pe=100, 1000 and 10000. Fig. 9 shows the mixing index according to the Péclet number for Fm=4, f=0.3 and Np=800. It is found that the best and fastest mixing can be achieved in the case of Pe =100. With decreasing Péclet number, the mixing index decreases, indicating the increase in the mixing performance. It is due to the smaller Péclet

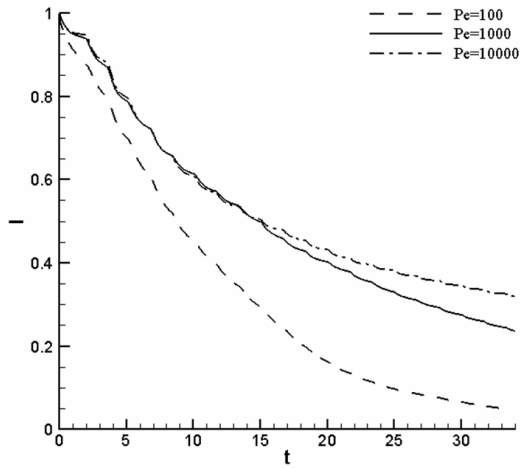

Fig. 9. Mixing index according to the Péclet number for F_m=4, f=0.3 and N_p=800.

number, which means the higher diffusion, leading to better mixing.

3.2.2 Effect of switching frequency

The variation of the mixing efficiency with the actuation frequency is investigated for 800 magnetic particles under an external magnetic force F_m=4. As the switching frequency increases, the distance the magnetic particles can travel over decreases. Note that the mixing performance is significantly influenced by the particle-traveling distance: when magnetic particles oscillate over longer distance, good mixing can be attained within shorter time of magnetic actuation. In case of the higher frequency, only a smaller number of magnetic particles can travel the whole channel (wall to wall), making it more difficult to create the chains of clustered particles for good mixing.

Fig. 10 shows the mixing index according to the switching frequency for F_m=4, N_p=800 and Pe=1000. From the figure, it is clear that, with increasing frequency, the mixing performance becomes more efficient (f<0.3) and then reaches maximum at f=0.3. It is due to the increase of the agitation number of magnetic particles with the frequency. For a frequency higher than the optimum (f>0.3), however, the performance becomes inefficient. Particularly, it becomes very poor for f>0.5. It is closely related to the particle clustering. That is, the probability of the particle clustering decreases because the possibility of collision between the particles and the walls becomes reduced due to the short actuation period.

Fig. 11 depicts the instantaneous magnetic particle distribution at t=23.2 in two cases of f=0.5 and f=0.6 for F_m=4, N_p=800 and Pe=1000. In the case of f=0.5, chains of magnetic particles are observed. In the case of f=0.6, however, they little appear, resulting in very poor mixing performance.

3.2.3 Effect of number of magnetic particles

As mentioned, the mixing process depends strongly on the chains of magnetic particles and the more chains can be cre-

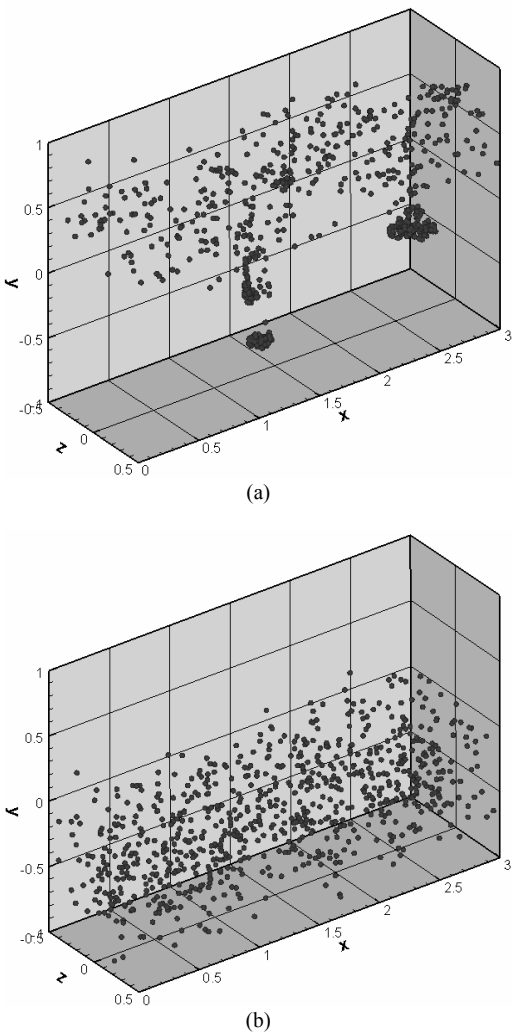

Fig. 11. Instantaneous particle distribution at t=23.2 for F_m=4, N_p=800 and Pe=1000: (a) f=0.5, (b) f=0.6.

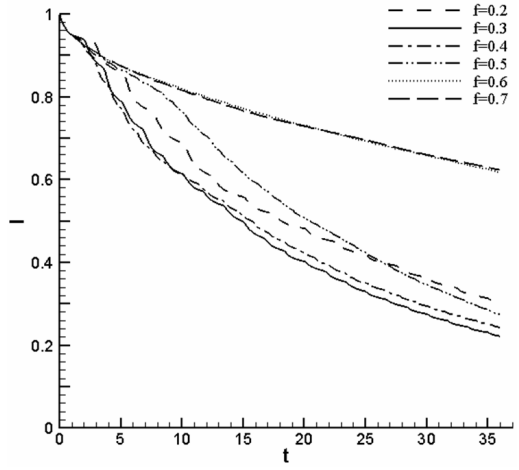

Fig. 10. Mixing index according to the switching frequency for F_m=4, N_p=800 and Pe=1000.

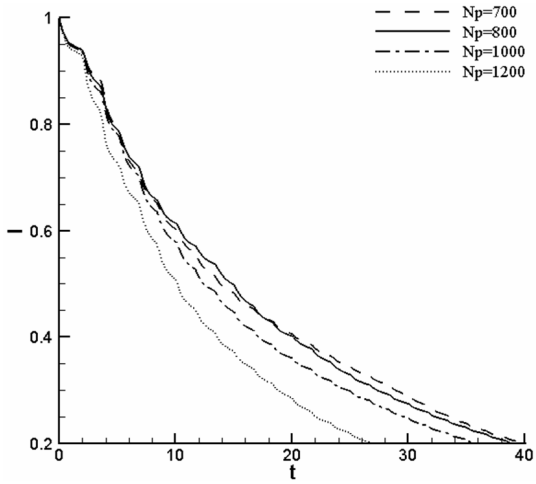

Fig. 12. Mixing index according to the magnetic particle number for F_m=4, f=0.3 and Pe=1000.

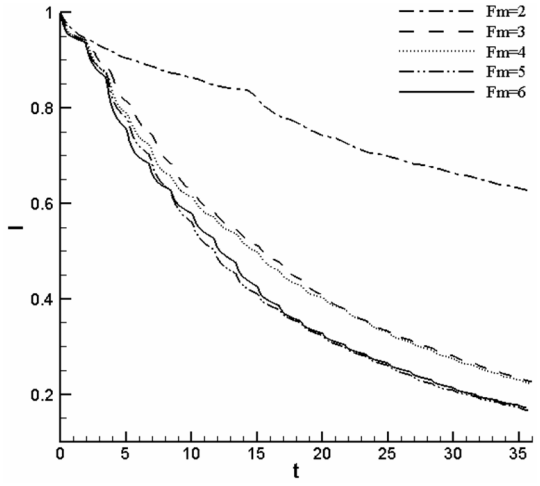

Fig. 13. Mixing index according to the magnetic-force magnitude for f=0.3, N_p=800 and Pe=1000.

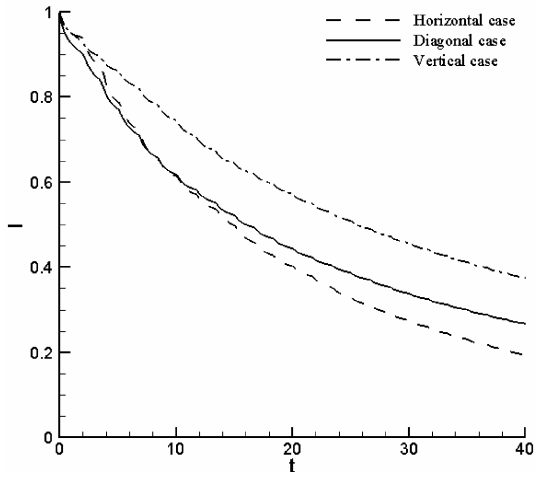

Fig. 14. Mixing index according to the initial scalar concentration for F_m=4, f=0.3, N_p=800 and Pe=1000.

ated by the more magnetic particles. To evaluate the effect of the number of magnetic particles, the optimum frequency f=0.3 for F_m=4, N_p=800 and Pe=1000 is considered; the mixing index according to the magnetic-particle number is shown in Fig. 12. Approximately 80% mixing performance [(1-I)× 100%] is obtained at t=27 for N_p=1200 particles, at t=36 for N_p=1000 particles and at t=39 for N_p=800 particles. Thus, better mixing is obtained when a larger number of magnetic particles are used,

3.2.4 Effect of magnitude of magnetic force

The magnetic-force magnitude and switching frequency are the main parameters that play important parts in the particle distribution. Fig. 13 shows the variation of the mixing index with the magnitude of magnetic force while fixing the switching frequency and the particle number at f=0.3 and N_p=800, respectively. As mentioned above, it is found that f=0.3 is the optimum frequency for the magnetic force F_m=4, but it is not optimal for all the other magnetic-force magnitudes, for instance F_m=2. With a small magnetic force, the particles travel only within a short distance and thus the enhancement of the mixing becomes limited like the case of high switching frequency. To improve the mixing efficiency for the small actuation magnetic force, a low operating frequency should be applied. In this way, magnetic particles have more opportunity to travel the entire vertical range and create the chains of magnetic particles. In other words, with the high magnetic-force magnitude, F_m=6 for instance, the mixing can be accelerated because the magnetic particles travel rapidly.

However, the time during which the particles stay at the walls becomes long, limiting the mixing efficiency like the case of low actuation frequency. Fig. 13 shows the optimum magnetic-force magnitude at F_m=5 for f=0.3, N_p=800 and Pe=1000, indicating the variation of the optimum frequency with the magnetic-force magnitude.

3.2.5 Effect of the initial condition

It is well known that the mixing also depends strongly on the initial distribution of the scalar concentration: for example, sample and buffer supplied into the channel. To estimate how much the initial condition affects the mixing performance, three simple cases are considered: horizontal, diagonal and vertical (see Fig. 5). Fig. 14 shows the mixing index according to the initial concentration distribution for F_m=4, f=0.3, N_p=800 and Pe=1000. The mixing rate, for the horizontal case where the initial interface between the sample and buffer is perpendicular to the magnetic force direction, is higher than those for the other two cases. With decreasing angle between the magnetic force and interface directions, the mixing efficiency is reduced. In other words, the mixing performance decreases in the order of horizontal, diagonal and vertical cases.

Fig. 15 shows the temporal evolution of the concentration distribution for N_p=800, F_m=4, f=0.3 and Pe=1000 in the horizontal, diagonal and vertical cases, indicating the strong dependence of the initial condition on the mixing. In all the cases, mixing is not made fully around the walls, particularly in the corners. From these figures, it can also be recognized that this kind of mixer is more suitable for the horizontal case than for the other ones.

4. Conclusions

By developing a numerical code based on finite volume method, we have investigated the characteristics of the flow and mixing in a micromixer using magnetic particles. Results show that the chains of the clustered magnetic particles, which are created and move up and down during the magnetic actuation, play an important part in the good mixing. The mixing behavior could be clearly observed in terms of the folding and stretching in the Poincaré sections with a cubic blob of 8000 passive fluid particles located initially at the center of the microchannel. By considering the various initial conditions of

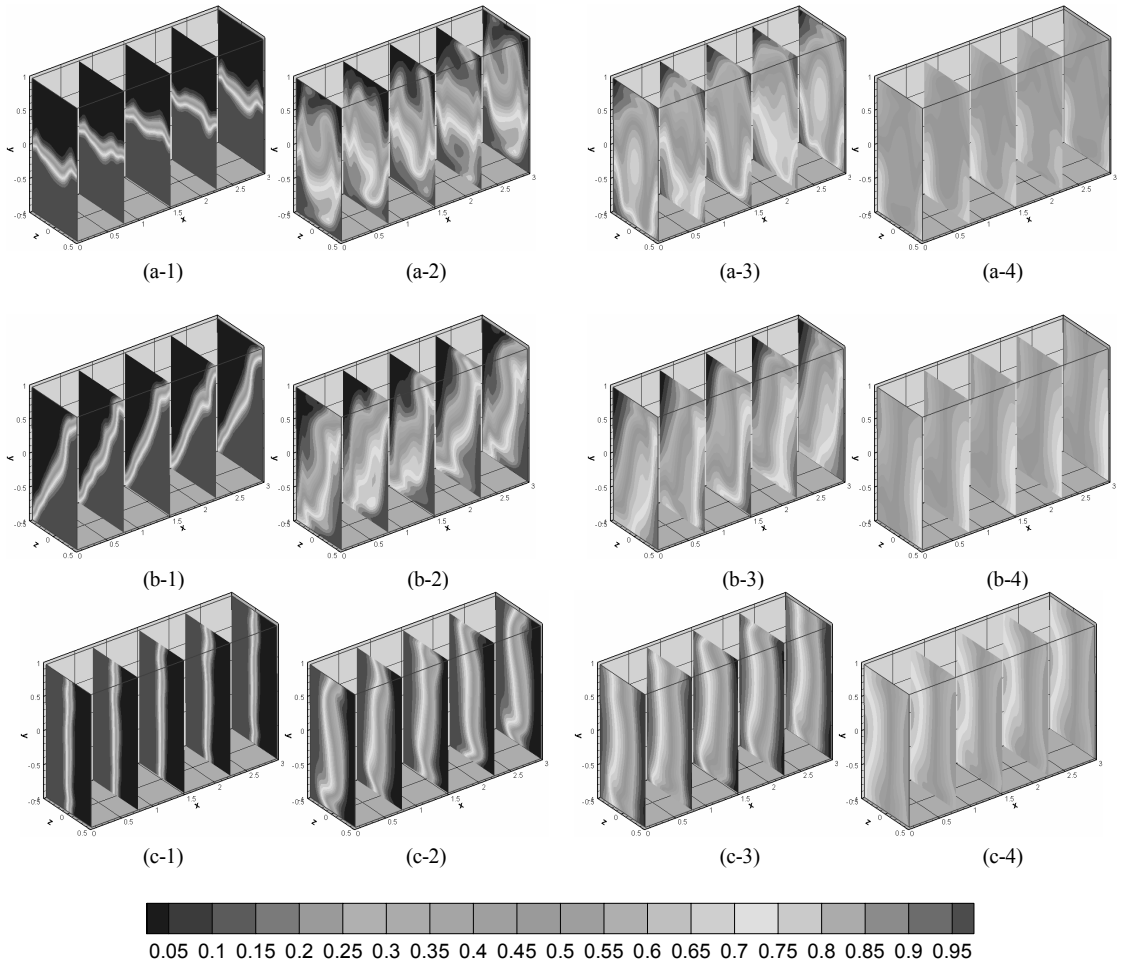

Fig. 15. Temporal evolution of the concentration distribution for N_p=800, F_m=4, f=0.3, (a) horizontal, (b) diagonal and (c) vertical cases at t= (1) 2, (2) 8, (3) 16, and (4) 40.

the concentration distribution, we propose that the mixer is most suitable for the horizontal concentration distribution where the initial interface between the sample and buffer is perpendicular to the magnetic force direction.

We also addressed the effect of the magnetic force magnitude and the switching frequency which have a combined influence on the mixing efficiency. The optimum frequency f=0.3 was obtained for the magnetic force magnitude F_m=4, while the optimum magnetic force F_m=5 was for the switching frequency f=0.3. It indicates that the optimum frequency depends strongly on the applied magnetic force for the best mixing and vice-versa.

Finally, the mixing was studied according to the magnetic particle number. The greater the number of magnetic particles that were used, the better mixing in the shorter time was obtained.

Acknowledgment

This work was supported by the National Research Foundation of Korea through the NRL Program funded by the Ministry of Education, Science and Technology (Grant No. 2005-1091).

Nomenclature

$C, \bar{C}$	:	Concentrations
D	:	Diffusion coefficient
F_d	:	Drag force
F_m	:	Magnetic force
f	:	Switching frequency of magnetic actuation
f_d	:	Drag force per unit mass
H	:	Half-height of microchannel
I	:	Mixing index
L	:	Periodic length of microchannel
m_p	:	Mass of magnetic particle
N	:	Total number of grid points
N_p	:	Number of magnetic particles
Pe	:	Péclet number
p	:	Pressure
Re	:	Reynolds number
R_p	:	Radius of magnetic particle
T	:	Period of magnetic actuation
t	:	Time
U_0	:	Average main-flow velocity
u_i	:	Velocity components of flow

$u_{p,i}$: Velocity components of magnetic particle
α, γ, ρ : Runge-Kutta coefficients
Δt : Time increment
ρ_f : Density of fluid
ρ_p : Density of magnetic particle
υ : Kinematic viscosity of fluid

Subscripts

i : Indices
f : Surrounding fluid
p : Particles

References

[1] V. Mengeaud, J. Josserand and H. H. Girault, Mixing processes in a zigzag microchannel: Finite element simulations and optical study, *Analytical Chemistry*, 74 (16) (2002) 4279-4286.

[2] A. Rida and M. A. M. Gijs, Manipulation of self-assembled structures of magnetic beads for microfluidic mixing and assaying, *Analytical Chemistry,* 76 (21) (2004) 6239-6246.

[3] H. Suzuki and C. M. Ho, A chaotic mixer for magnetic bead-based micro cell sorter, *Journal of Microelectromechanical Systems*, 13 (5) (2004) 779-790.

[4] M. Zolgharni, S. M. Azimi, M. R. Bahmanyar and W. Balachandran, A numerical design study of chaotic mixing of magnetic particles in a microfluidic bio-separator, *Microfluidics and Nanofluidics*, 3 (6) (2007) 677-687.

[5] Y. Wang, J. Zhe, B. T. F. Chung and P. Dutta, A rapid magnetic particle driven micromixer, Springer, *Microfluidics and Nanofluidics*, 4 (5) (2008) 375-389.

[6] D. W. Oh, J. S. Jin, J. H. Choi, H. Y. Kim and J. S. Lee, A microfluidic chaotic mixer using ferrofluid, *Journal of Micromechanics and Microengineering*, 17 (10) (2007) 2077-2083.

[7] F. Carlsson, M. Sen and L. Lofdahl, Fluid mixing induced by vibrating walls, *European Journal of Mechanics-B/Fluids*, 24 (3) (2005) 366-378.

[8] J. R. Pacheco, K. P. Chen and M. A. Hayes, Rapid and efficient mixing in a slip-driven three-dimensional flow in a rectangular channel, *Fluid Dynamics Research,* 38 (8) (2006) 503-521.

[9] X. Niu and Y. K. Lee, Efficient spatial-temporal chaotic mixing in microchannels, *Journal of Micromechanics and Microengineering,* 13 (3) (2003) 454-462.

[10] Q. A. Pankhurst, J. Connolly, S. K. Jones and J. Dobson, Applications of magnetic nanoparticles in biomedicine, *Journal of Physics D: Applied Physics*, 36 (13) (2003) R167-R181.

[11] E. P. Furlani, Y. Sahoo, K. C. Ng, J. C. Wortman and T. E. Monk, A model for predicting magnetic particle capture in a microfluidic bioseparator, *Biomedical Microdevices* 9 (4) (2007) 451-463.

[12] N. Pamme and A. Manz, On-chip free-flow magnetophoresis: Continuous flow separation of magnetic particles and agglomerates, *Analytical Chemistry*, 76 (24) (2004), 7250-7256.

[13] P. Gondret, N. Rakotomalala, M. Rabaud, D. Salin and P. Watzky, Viscous parallel flows in finite aspect ratio Hele-Shaw cell: Analytical and numerical results, *Physics of Fluids* 9 (6) (1997), 1841-1843.

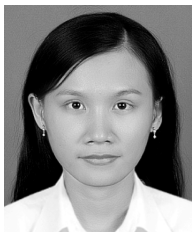

Thanh Nga Le received her B.S. in Aeronautical Engineering from Ho Chi Minh City University of Technology, Vietnam, in 2007. She then received her M.S. degree in Mechanical Engineering from Dong-A University in Busan, Korea, in 2009. And now, she is working for Capital and Commercial Limited in Vietnam.

Yong Kweon Suh received his B.S. in Mechanical Engineering from Seoul National University, Korea, in 1974. He then received his M.S. and Ph.D. degrees from SUNY Buffalo in 1985 and 1986, respectively. Dr. Suh is currently Professor at the Department of Mechanical Engineering at Dong-A University in Busan, Korea. His research interests include electrokinetic phenomena such as electro-osmosis, electrophoresis, motion of magnetic particles, and mixing in micro/nano scales.

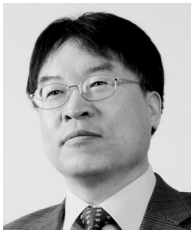

Sangmo Kang received B.S. and M.S. degrees from Seoul National University in 1985 and 1987, respectively, and then worked for five years in Daewoo Heavy Industries as a field engineer. He also achieved Ph.D. in Mechanical Engineering from the University of Michigan in 1996. Dr. Kang is currently Professor at the Department of Mechanical Engineering at Dong-A University in Busan, Korea. Dr. Kang's research interests are in the area of micro- and nanofluidics and turbulent flow combined with the computational fluid dynamics.